29th International Cosmic Ray Conference Pune (2005) **00**, 101-104

The EGRET sky: a new interstellar emission model and source detection

J.M. Casandjian[a], I. Grenier[a], R. Terrier[b]
(a) AIM (CEA/Paris 7/CNRS),UMR 7158, Service d'Astrophysique, CEA Saclay, 91191 Gif/Yvette, France
(b) APC (Paris 7/CNRS/CEA),UMR 7164,11 place Marcelin Berthelot, 75005 Paris, France
Presenter: J.M. Casandjian (casandjian@cea.fr), fra-casandjian-J-abs1-og21-oral

The comparison of HI, CO, dust, and gamma-ray maps in the solar neighborhood has led to the discovery of large amounts of dark gas. The large mass and angular extent of the local dark clouds, as well as their clumpiness, imply severe revisions of the interstellar emission model to high latitudes, therefore of the detectability of a point-source above the diffuse background. We have used this new model to search for point-like sources at $5° \leq |b| \leq 80°$ and we show that numerous persistent unidentified EGRET sources are not confirmed as significant sources.

1. Introduction

During its nine years of operation the EGRET detector on board the *Compton Gamma Ray Observatory* has recorded gamma rays from 30 MeV to over 20 GeV in energy. The third EGRET catalogue (3EG) was published [1] from the data taken between April 1991 and October 1995 (P1234). 271 point-like sources were found above the interstellar model of Hunter et al. [2]. Among them, only 72 were firmly identified as blazars or pulsars. The remaining 197 unidentified sources have been extensively studied, individually or collectively. Their variability, energy spectra, multi-wavelength counterparts, and spatial distribution were analyzed [3]. A significant correlation with the Gould Belt was suggested for the persistent sources [4,5,6] leading to a decomposition into at least three classes: bright sources a few kpc away in the Galactic disc, faint local sources associated with the Gould Belt, and extragalactic sources.

Since the Galactic and extragalactic diffuse emissions contribute about 90% of the EGRET photons, the knowledge of the gas content of the Galaxy and its radiation field is crucial for the source detection. A precise model is needed to accurately determine the number, position and flux of the sources. The recent comparison of interstellar gas tracers in the solar neighborhood (HI and CO lines from the atomic and molecular gas, dust thermal emission, and γ rays from cosmic-ray interactions with gas) has unveiled vast clouds of cold dust and dark gas [7]. Cosmic rays in the dark gas radiate in gamma rays through pion production and decay as well as bremsstrahlung. A new interstellar emission model has been developed to include this new gas component.

2. Interstellar emission

Assuming energetic cosmic rays uniformly penetrate all gas phases in the local interstellar medium, within a kpc, the γ-ray intensity in each direction can be modeled as a linear combination of gas column-densities (HI, H_2 from CO, and dark gas), the Galactic inverse Compton intensity, and an isotropic extragalactic background intensity. The predicted map in photon counts, with the different component emissivities as free parameters, is fitted to the γ-ray data using a maximum-likelihood test with Poisson statistics [7,8]. The N(HI) column-densities come from the recent Leiden/Argentina/Bonn HI data cube for a spin temperature of 120 K [9,10,11,12], and the velocity-integrated W(CO) brightness temperature map from the CfA compilation [13,14]. The dust reddening E(B-V) map comes from the 100μm and 240μm data from IRAS and DIRBE

after correction to a uniform temperature of 18.2 K [15]. As a template for the dark gas, we have used residual dust maps after removal of the E(B-V) part linearly correlated with N(HI) and W(CO) [7]. The inverse Compton map was calculated with GALPROP 45-600202. Emission from energetic electrons in the nearby radio loops is traced by the 408 MHz synchrotron map [16]. More information is given in the companion paper [8]. The validity of this model is limited to $|b| \geq 5°$ [7]. The longitude and latitude distribution displayed in Figure 1 illustrate the very good fit to the EGRET data above 100MeV.

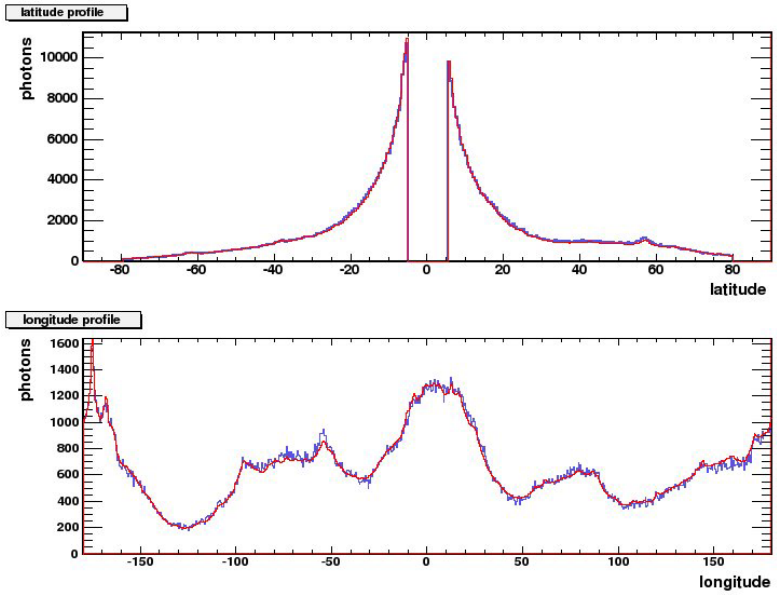

Figure 1. Latitude and longitude distributions of the EGRET photons above 100MeV. The EGRET data are in blue, our new diffuse model in red.

3. Source detection

To evaluate the impact of the dark gas on source detection and on the results of the 3EG catalogue, we have used a detection method as close as possible to that of the catalogue. There are, however, slight differences. The catalogue positions are extracted from the viewing period in which the source was most significantly detected whereas we obtain it from the cumulative P1234 map. The data itself have slightly changed. We have used the counts and exposure maps available from the CGRO Science Support Center that were reprocessed after the catalogue publication. We have used the same likelihood code LIKE [17] for source detection as that used for the catalogue. We concentrate here on the *persistent* sources, namely those significantly detected ($\geq 5\sigma$ at $|b| < 10°$, $\geq 4\sigma$ at $|b| \geq 10°$) in the cumulative P1234 data.

The spectral indices of the three strongest sources, the Crab, Geminga and Vela pulsars, were respectively set to 2.1, 1.5 and 1.7 and to 2.0 for all the other sources. We divided the cartesian (l,b) map in 18 regions to search for point-like sources. For each region a likelihood test statistics (TS) map was computed. Significant excesses ($\geq 3\sigma$) were analyzed iteratively, starting for the most significant one. An excess position is first calculated from the centroid of the 50% confidence ellipse around the TS peak. For this source and all those previously detected within 20 degrees of this one, a position and flux optimization iteration was performed. This procedure was used in a loop until no excess above 2.5 σ were left. Reducing the detectability threshold decreases the risk of having a weak source shadowed by a stronger closeby neighbour. Once all the sources in

a region were found, we removed the sources with TS < 3σ and recalculated iteratively the flux for all the others. At this stage, source positions were calculated from the centroid of the 95% confidence ellipse.

Then all the sources from the 18 regions were merged and a flux optimization was performed for the whole sky map to take into account the mutual influence of sources close a region border. The importance of this step is lowered by the fact than in the individual source detections, sources previously detected just outside the region borders were also included. At the end of the procedure, a global TS map was calculated to verify that no excess above 3σ was left. This procedure was repeated at energies >100MeV, 300MeV-1GeV, and >1GeV and we used the most accurately determined position and optimized the flux above 100MeV at this given position. At |b| > 60°, the same procedure was used in equatorial coordinates (for E>100 MeV only).

4. Evaluation of the method

To evaluate our method, we have first used the same interstellar emission model at all latitudes as for the 3EG catalogue. Our analysis yields 169 persistent sources with a detection significance above 5σ at |b|<10° and 4σ at higher latitude. The 3EG catalogue lists 174 persistent ones with the same criterion, but 18 of them, very near the detection threshold, have dropped below the threshold in the new analysis or moved to a position outside the error box. Conversely, we have found 18 significant sources that are not listed or have a different position in the EGRET catalogue. To compare positions, we have used a match test with a completeness of 99%. If we release this criterion and allow a slight shift in position, the number of 3EG sources without a match falls to 11, among which 9 were statistically weak excesses, only 0.5 σ above the threshold.

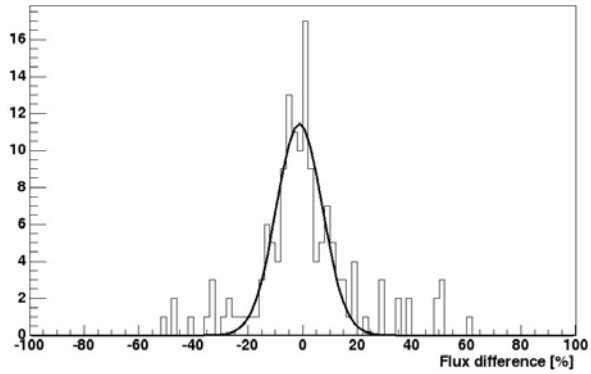

Figure 2. Relative flux difference between the 3EG and present estimates for persistent sources in cycles 1-4 at energies E > 100MeV. The Gaussian curve that best fits the distribution has an 8% dispersion.

Figure 2 shows the relative flux difference for the persistent sources between the 3EG and our estimate. This difference can be mainly attributed to the data reprocessing by the EGRET team after the catalogue was published. We indeed obtain the same distribution when we measure the 3EG source fluxes at their catalogued position with the new photons and exposure maps.

In conclusion, our method compares well with the 3EG analysis. Most of the sources were found at a consistent position and within 20% in flux. The only differences between the two source lists arise very near the detection threshold where flux variations from the reprocessed data make several sources move up or drop below the threshold. A few sources were found at a different position.

5. Results

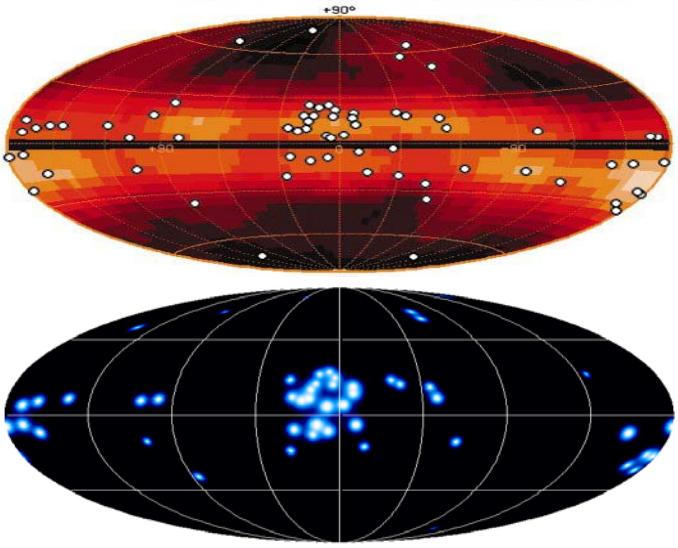

The same automatic procedure has been applied to the data at 5°<|b|<80° using the diffuse emission model described above instead of the EGRET one. We have found 96 persistent sources with a detection significance above 5σ at |b|<10° and 4σ at higher latitude, whereas 129 ones are given in the 3EG catalogue in this latitude range. 19 new significant sources do not have a 3EG counterpart and 49 3EG persistent sources did not pass the detection threshold in the new analysis or were found at a different position. A dozen of the latter are not confirmed in the new analysis because of the reprocessed data, the rest because of the impact of the nearby dark clouds. It is worth noting that 43 or the 49 unconfirmed 3EG sources were catalogued as unidentified (6 marginal AGN and 39 with no interesting counterpart) and only 6 were noted as firm AGN. Even though these sources do not pass the present detectability criterion, they might still exist or the alignment with a blazar just happened by chance coincidence.

Figure 3. Distributions (in Galactic coordinates) of (a) the 67 persistent unidentified 3EG sources at |b|>2.5° and the Gould Belt [5]; (b) the 49 3EG persistent sources at |b|>5° that do not pass the detection criteria with the new diffuse emission model including the nearby dark clouds.

Figure 3 shows the proposed association between the Gould Belt and the 67 persistent 3EG sources with no firm or marginal AGN counterpart [5]. Below are the 49 persistent 3EG sources that are not confirmed against the new interstellar emission model. The figure illustrates that most of the 3EG sources associated with the Belt in fact correspond to the emission borne in the clumpy dark clouds that surround all the molecular clouds of the nearby Gould Belt [7]. The possibility of a failure of the EGRET interstellar model had been proposed in 1995 to explain the source correlation with the local clouds [4], but it was later discarded because the large masses required to match the source fluxes could not have been missed in the HI, CO or IR surveys. It turns out that Nature does hide that much mass around the CO clouds. The dark gas detection is not simply the superposition of these sources. It was found with a huge significance on top of all the 3EG sources, including the Gould Belt ones that were trying to compensate for it [7]. The gamma radiation of the dark clouds, however, is bright enough to significantly lower a source detectability in their direction.

6. Conclusion

We have searched for point-like sources in the cumulative EGRET data between April 1991 and October 1995. To do so, we have developed a procedure based on the LIKE tool that we have first applied to the data with the same background model as for the 3rd EGRET catalogue, then with an interstellar emission model that includes the local dark clouds. A good agreement is found with the 3EG catalogue in the first case, small differences appearing because of the data reprocessing that took place in 2001. With the new interstellar background, only several new sources appeared and most of the persistent unidentified sources associated with the Gould Belt lost their significance.

References

[1] R.C. Hartman et al., Astrophys. J., Suppl. Ser., 123, 79 (1999).
[2] S.D. Hunger et al., Astrophys. J. 481, 205 (1997).

[3] P.L. Nolan et al., Astrophys. J. 597, 615 (2003) and references therein.
[4] I.A. Grenier, Advances in Space Research, vol. 15, n°5, 573, (1995).
[5] I. A. Grenier, Astronomy and Astrophysics, 364, L93 (2000).
[6] N. Gehrels et al., Nature, 404, 363 (2000).
[7] I. A. Grenier et al., Science, 307, 1292 (2005).
[8] I. A. Grenier et al., in this volume.
[9] P.M.W. Kalberla et al., A&A, in press (astro-ph/0504140).
[10] Hartmann & Burton 1997, Cambridge University Press, ISBN 0521471117.
[11] E. Bajaja et al., A&A, in press (astro-ph/0504136).
[12] Arnal, E. M., Bajaja, E., Larrarte, J. J., Morras, R., & Pöppel, W. G. L. 2000, A&AS, 142, 35.
[13] T. M. Dame et al., Astrophys. J. 547, 792 (2001).
[14] T. M. Dame, P. Thaddeus, in Milky Way Surveys: The Structure and Evolution of Our Galaxy, D. Clemens, T. Brainerd, Eds. (ASP Conference Series, Astronomical Society of the Pacific, San Francisco, CA, 2004), pp. 66–72.
[15] D. J. Schlegel et al., Astrophys. J. 500, 525 (1998).
[16] C.G.T. Haslam et al, Astronomy and Astrophysics Supplement Series, 47, 1, (1982).
[17] J.R. Mattox et al., Astrophys. J, 461, 396 (1996).